Applied Numerical Modeling in Geomechanics – 2020 – Billaux, Hazzard, Nelson & Schöpfer (eds.) *Paper: 06-03*
©2020 Itasca International, Inc., Minneapolis, ISBN 978-0-9767577-5-7

Modelling the water injection induced fault slip in an argillaceous rock

W.J. Shiu, W.C. Chang & F.Y. Hsiao
SINOTECH Engineering Consultants, Inc., Taipei, TAIWAN

1 INTRODUCTION

Fault reactivation is one of the major issues related to the safety of deep geological disposal for radioactive waste. Risk may arise when fault reactivation is triggered, leading to an increase in permeability and a potential pathway for radionuclide transportation. It has been reported that the key factors dominating the fault slip are shear stress and the magnitude of frictional resistance (Lisle & Srivastava 2004). Different models for reproducing the behavior of fault reactivation have been proposed (Tsopela et al. 2016, Nguyen et al. 2019). However, the understanding of relevant hydro-mechanical response to fault reactivation is still limited. A conventional approach to trigger the fault reactivation, and thereafter crack propagation, is to inject water into a fractured rock mass. In the present work, a *3DEC* model (Itasca 2013) is used to reproduce the behavior of the fault reactivation. The numerical configuration is set based on the data obtained from experiments carried out at Mont Terri underground research laboratory (Guglielmi et al. 2015, Guglielmi et al. 2017). Mechanical response of the fault is simulated by Coulomb Slip material, whereas two flow models are used to reproduce hydraulic behavior of different nature of the fault. A fully coupled hydro-mechanical calculation, used for the present study, is based on the fast-flow logic implemented in *3DEC*.

2 MODEL DESCRIPTION

A simple model geometry is used for this study: a cube of 20 m length representing the host rock with a single fracture of 65° dip angle. In order to better reproduce the model behavior during water injection induced fault reactivation, a smaller mesh size (0.25 m) is used for zones located close to the fault whereas a gross mesh is used when moving away from the fault. Table 1 gives the relevant parameters used for fault, rock and fluid. Note that the host rock is assumed to be elastic and impermeable. Thus, fluid flow is only allowed on the fault plane. Two fault models are studies (referred as FM1 and FM2 in Table 1):

- FM1: Fluid flow takes place between two elements where mechanical failure is detected (according to Coulomb slip failure criteria). In order to allow the fluid flow to take place during the early injection period, some initial cracks are introduced around the injection point within a circle of 0.5 m radius. Note that, elements located beyond this predefined region are intact contacts. Thus, no fluid flow is allowed at the outer region before formation of new cracks. This flow model can be used to simulate a fault with filling material.
- FM2: Fluid flow goes freely over the entire flow plane without regarding the failure status of elements. This flow model can be used to simulate an already opened fault.

For the joint fluid flow computation, we assume that the flow goes through two parallel plates. The distance between these two plates is hydraulic aperture, u_h. The flow rate, q_i, per unit width of the plates may be written by the cubic law (Witherspoon et al. 1980):

$$q_i = -\frac{u_h{}^3 \rho g}{12\mu} \emptyset_{,i} = -k_H \emptyset_{,i} \quad (1)$$

Where μ is the fluid viscosity, ρ is the fluid density, g is the gravity acceleration, $\emptyset_i$ is the hydraulic head, and k_H is the hydraulic conductivity.

Table 1. Parameters for Fault, Host Rock and Fluid.

Material	Parameter	Value	
		FM1	FM2
Fault (Elasto-Plastic)	Normal Stiffness, kn (GPa/m)	20	20
	Shear Stiffness, ks (GPa/m)	20	20
	Cohesion (MPa)	0	0
	Friction Angle (°)	22	22
	Dilation Angle (°)	0	10
	Tensile Strength (MPa)	0	0
	Initial Aperture (μm)	28	10
Host Rock (Elastic)	Bulk Modulus, K (GPa)	5.9	5.9
	Shear Modulus, G (GPa)	2.3	2.3
	Density (kg/m3)	2450	2450
	Permeability	0	0
Fluid	Density (kg/m3)	1000	1000
	Compressibility (Pa-1)	4.4E-10	4.4E-10
	Viscosity (Pa s)	1E-3	1E-3

3 RESULTS AND DISCUSSION

Results of FM1 and FM2 simulations are compared in Figure 1, in terms of stress patterns and displacement. During the stepwise injection test, the increase in pore pressure (curve in gray) yields a decrease in effective normal stress (curve in blue). The “maximum shear stress” (curve in green) can be further computed using Coulomb slip criteria, *i.e.*, the resistance in shear is proportional to normal stress and friction angle. The fault slip is trigged when the maximum allowable shear stress (denote as “max shear stress” in Fig. 1) is dropped to the same magnitude as the in-situ shear stress (curve in red). For FM1 model, the slip is triggered at approximately 420 seconds. At that time, a significant increase in shear displacement along dip direction is observed (see Fig. 1 right). Note that, no shear displacement along strike is produced, since the movement of the joint shear displacement is dominated by the orientation of in-situ shear stress of the joint.

Due to the different concept of fluid flow logic used for FM1 and FM2 models, the pore pressure contour behaves in a very different way (see Fig. 2). For FM1 model, the fluid flow is initially limited within a small region around the injection point. The crack propagation takes place at 420 seconds. The allowable fluid flow region is expanded from 0.5 m radius to 4.8 m radius over the next 30 seconds. For FM2 model, the fluid flow is leaked out over the entire flow plane, resulting in a smaller average pore pressure around the injection point. A higher flow rate at the injection point can be expected for FM2 model to keep the pore pressure as the prescribed one. Stress evolutions at the injection point are illustrated on Figure 1. Similar stress drop is observed for FM1 (solid curves) and FM2 (dotted curves). Logically, the same normal displacement is produced (right of Fig. 1). However, shear displacement produced by FM1 model is much higher than for FM2 model. For FM1 model, the injected water is cumulated within a small region. The pore pressure for elements inside this region is synchronously increasing, leading to a low average normal stress. Fault slip is firstly occurred at the injection point. Thereafter, shear failure is quickly expanded around the injection point. A regional scale of fault slip is triggered, resulting in a pronounced shear displacement. For FM2 model, a lower shear displacement is produced since limited increase in pore pressure is observed. It seems that the model response predicted by FM1 fits better the observation from Mont Terri experiment test.

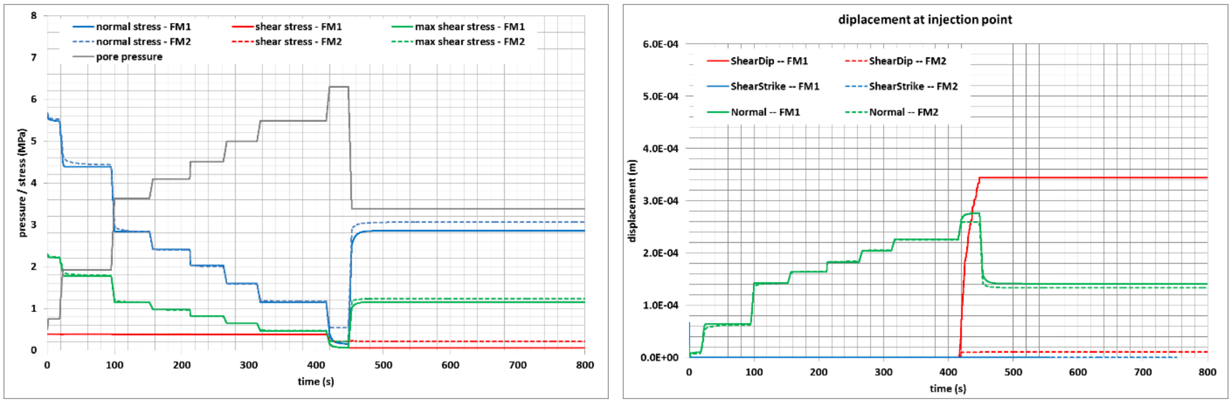

Figure 1. Evolution of stress patterns (left) and displacement (right) at the injection point.

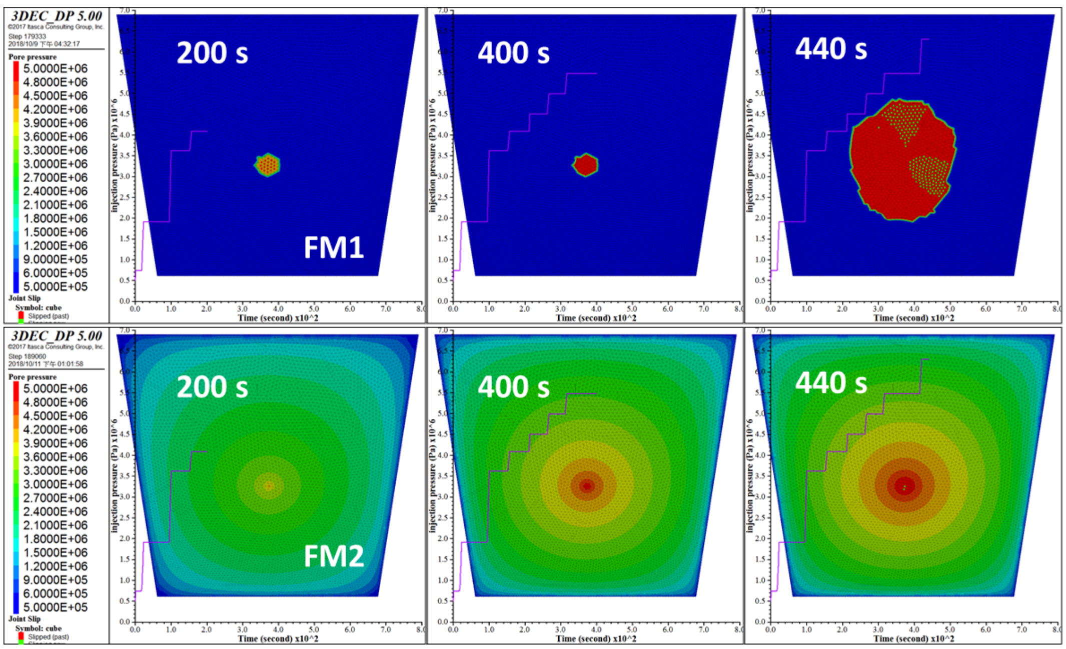

Figure 2. Pore pressure contour on the flow plane for FM1 and FM2.

4 CONCLUSIONS

The present study is aimed at reproducing the water injection induced fault slip in an argillaceous rock. A *3DEC* conceptual model with simple geometry is proposed to simulate the behavior of the fault reactivation. The numerical configuration is set based on the data obtained from experiments carried out at Mont Terri URL. The mechanical response of the joint is modeled by Coulomb slip criteria. Two joint flow models are used for simulating hydraulic behavior of different nature of fault: fault with filling material (FM1) and fault considered as already opened (FM2). The key factors dominating the fault slip are joint shear strength and *in-situ* stress. It shows that as the injection pressure increases, the effective stress near the injection point decreases, leading to slip failure. Both models correctly predict the previous fault reactivation process, with different magnitudes of shear displacement. For FM1 model, the injected water is cumulated near the injection point. High pore pressure is developed and a regional fault reactivation is observed, resulting in obvious shear displacement around the injection point. For FM2 model, the increase in pore pressure is limited due to the water leakage through the entire flow plane. As a consequence, only a small amount of shear displacement is produced.

The present work shows reasonable results of a fully coupled fault reactivation process by using a rather simple model geometry. The model can be used to evaluate the potential of a problematic fault slip by adjusting adequately the flow model. Future work will be focus on the evolution of the permeability of the fault after the on-set of fault reactivation.

REFERENCES

Guglielmi, Y., Birkholtzer, J., Rutqvist, J., Jeanne, P. & Nussbaum, C. 2017. Can Fault leakage occur before or without reactivation? Results from an in-situ reactivation at Mont Terri. *Energy Procedia*, 114, 3167-3174.

Guglielmi, Y., Cappa, F., Lançon, H., Janowczyk, J.B., Rutqvist, J., Tsang, C.E. & Wang, J.S.Y. 2013. ISRM Suggested Method for Step-Rate Injection Method for Fracture In-Situ Properties (SIMFIP): Using a 3-Components Borehole Deformation Sensor. *Rock Mech. Rock. Eng.* 47, 303-311.

Guglielmi, Y., Elsworth, D., Cappa, F., Henry, P. Gout, C., Dick, P. & Durand, J. 2015. In-situ observations on the coupling between hydraulic diffusivity and displacements during fault reactivation in shales*, J. Geophys. Res. Solid Earth*, Vol. 120, No. 11, pp. 7729-7748.

Itasca Consulting Group, Inc. 2013. *3DEC – 3-Dimensional Distinct Element Code, Ver. 5.0*. Minneapolis: Itasca.

Lisle, R.J. & Srivastava D.C. 2004. Test of the frictional reactivation theory for faults and validity of fault-slip analysis, *Geology*, Vol. 32, No. 7, pp. 569-572.

Nguyen, T.S., Guglielmi, Y., Graupner, B. & Rutqvist, J. 2019. Mathematical modelling of Fault Reactivation Induced by Water Injection. *Mineral*, 9. 282.

Tsopela, A., Donzé, F. V., Guglielmi, Y., Castilla, R. & Gout, C. 2016. Hydro-mechanical modelling of hydraulic injection inside a fault zone, *50th US Rock Mechanics / Geomechanics Symposium in Houston, Texas USA 26-29 June, ARMA* 16-476.

Witherspoon, P.A., Wang J.S.Y., Iwai, K. & Gale, J.E. 1980. Validity of Cubic Law for Fluid Flow in a Deformable Rock Fracture. *Water Resource Res.,* 16(6), 1016-1024.